Antiviral Research 108 (2014) 65–73

Contents lists available at ScienceDirect

Antiviral Research

journal homepage: www.elsevier.com/locate/antiviral

Inhibition of adenovirus replication by a trisubstituted piperazin-2-one derivative

Javier Sanchez-Cespedes [a,1], Crystal L. Moyer [a], Landon R. Whitby [b], Dale L. Boger [b], Glen R. Nemerow [a,*]

[a] Department of Immunology and Microbial Science, The Scripps Research Institute, 10550 N. Torrey Pines Road, Mailcode IMM4, La Jolla, CA 92037, USA
[b] Department of Chemistry, The Scripps Research Institute, 10550 N. Torrey Pines Road, Mailcode BCC483, La Jolla, CA 92037, USA

ARTICLE INFO

Article history:
Received 22 October 2013
Revised 15 May 2014
Accepted 19 May 2014
Available online 4 June 2014

Keywords:
Adenovirus
Antiviral compound
DNA replication inhibitor

ABSTRACT

The number of disseminated adenovirus (Ad) infections continues to increase mostly due to the growing use of immunosuppressive treatments. Recipients of solid organ or hematopoietic stem cell transplants, mainly in pediatric units, exhibit a high morbidity and mortality due to these infections. Unfortunately, there are no Ad-specific antiviral drugs currently approved for medical use. To address this situation, we used high-throughput screening (HTS) of synthetic small molecule libraries to identify compounds that restrict Ad infection. Among the more than 25,000 compounds screened, we identified a hit compound that significantly inhibited Ad infection. The compound (15D8) is a trisubstituted piperazin-2-one derivative that showed substantial antiviral activity with little or no cytotoxicity at low micromolar concentrations. Compound 15D8 selectively inhibits Ad DNA replication in the nucleus, providing a potential candidate for the development of a new class of antiviral compounds to treat Ad infections.

1. Introduction

Human adenoviruses (Ads) are non-enveloped viruses consisting of more than 60 serotypes divided into 7 subgroups or species (A–G) (Robinson et al., 2013). These viruses are responsible for diseases ranging from acute respiratory and ocular infections to more severe enteric diseases, but are rarely associated with severe clinical symptoms in otherwise healthy individuals (Echavarria, 2008; Tebruegge and Curtis, 2012). However, the growing implementation of immunosuppressive therapies together with the improvement of viral diagnostic tools has revealed Ad to be one of the more common causes of potentially life-threatening viral diseases associated with transplantation and a leading cause of increased infections in pediatric units (Echavarria, 2008; Razonable and Eid, 2009). Ad infections occur in frequencies between 3–47% in pediatric allogeneic hematopoietic stem cell transplant (HSCT) recipients with associated mortality rates of 2–80% (Echavarria, 2008; Verdeguer et al., 2011). Ad infections occur in approximately 10% of liver and heart transplant recipients, and in 22% of lung recipients (Humar et al., 2005; Ison and Green, 2009). Despite the significant clinical impact, there are no currently approved antiviral therapies for Ad infections. Sub-optimal therapeutic options to treat Ad infections in immunosuppressed patients include the use of broadly acting antivirals such as ganciclovir, acyclovir, vidarabine, ribavirin and cidofovir, with highly variable results (Lenaerts et al., 2008). Ribavirin and cidofovir are the most frequently used, however, neither has been approved for specific use in Ad infections. Ribavirin has variable activity against different Ad types, displaying maximum activity against subgroup C; however, the plasma concentrations reached by ribavirin are 10 times below the required IC_{50} value (Morfin et al., 2005, 2009). On the other hand, cidofovir exhibits antiviral activity against all Ad species but has low oral bioavailability, significant toxicity (tubular necrosis), and does not confer long term protection (Lindemans et al., 2010). While a lipidic conjugate of cidofovir, CMX001, is currently being tested in a Phase II clinical trial (Paolino et al., 2011; Toth et al., 2008) other potential antiviral agents with increased therapeutic activity are still needed.

Small chemically-derived molecules with potent antiviral activity can be selected from large and diverse chemical libraries to derive new classes of antiviral drugs (Cianci et al., 2004; Este and Telenti, 2007; Frey et al., 2006; Plemper et al., 2004). The main objectives of the current study were to identify molecules derived from synthetic small molecule libraries that restrict Ad infection and determine their mechanism of action as a first step in the development of a new and specific anti-Ad therapy.

* Corresponding author. Tel.: +1 (858) 784 8072; fax: +1 (858) 784 8472.
E-mail address: gnemerow@scripps.edu (G.R. Nemerow).
[1] Present address: Institute of Biomedicine of Seville (IBiS), University Hospital Virgen del Rocío/CSIC/University of Seville, Unit of Infectious Diseases, Microbiology and Preventive Medicine, Sevilla, Spain.

http://dx.doi.org/10.1016/j.antiviral.2014.05.010
0166-3542/

2. Material and methods

2.1. Chemical libraries

The combinatorial chemical libraries were generated by parallel synthesis utilizing solution-phase synthetic techniques as previously described (Boger et al., 1996; Cheng et al., 1996). The multistep synthesis of the chemical libraries employing liquid–liquid and liquid–solid extractions to remove unreacted starting materials, reagents, and reagent byproducts provided the purified final products (>95% pure) irrespective of reaction efficiency. Implementation was in formats for the parallel synthesis of individual pure compounds (100–1000 member libraries, individual compounds) and modest sized libraries composed of mixtures (8000-membered libraries, 10–20 compounds/mixture), an approach compatible with our screening. Notably, a number of effective small molecule modulators of protein–protein (Boger et al., 2003; Whitby et al., 2011; Whitby and Boger, 2012) or protein–DNA interactions (Stover et al., 2009) have been identified from screening these libraries.

2.2. Cells and virus

Human A549, 293 and MRC-5 cell lines were from the American Type Culture Collection (ATCC, Manassas, VA). The 293β5 stable cell line overexpressing the human β5 integrin subunit was generated by transfecting a cytomegalovirus promoter-driven expression plasmid containing the human β5 gene into 293 cells and selecting for neomycin resistance (Nguyen et al., 2010). These cell lines were propagated in Dulbecco's modified Eagle medium (DMEM, Life Technologies/Thermo Fisher) supplemented with 10% fetal bovine serum (FBS) (Omega Scientific, Tarzana, CA), 10 mM HEPES, 4 mM L-glutamine, 100 units/ml penicillin, 100 μg/ml streptomycin, and 0.1 mM non-essential amino acids (complete DMEM).

Wild-type Ad5 and Ad16 and HCMV (AD169) were obtained from ATCC. The Ad5-GFP and Ad16-GFP used in this work are replication-defective viruses containing a CMV promoter-driven enhanced green fluorescent protein (eGFP) reporter gene cassette in place of the E1/E3 regions (Nepomuceno et al., 2007). Ad viruses were propagated in 293β5 cells and isolated from cellular lysate by cesium chloride density centrifugation. Virus concentration, in mg/ml, was calculated with the Bio-Rad Protein Assay (Bio-Rad Laboratories) and converted to virus particles/ml (vp/ml) using 4×10^{12} vp/mg. HCMV was kindly provided by P. Romero-Perez (Institute of Biomedicine of Seville (IBiS), Sevilla, Spain).

2.3. High-throughput screening (HTS) of combinatorial chemical libraries

An initial rapid screening was performed using human A549 epithelial cells (3×10^5 cells/well in Corning black wall, clear bottom 96-well plates) infected with Ad5-GFP or Ad16-GFP (2000 vp/cell) in the presence of 50 μM of the candidate antiviral compounds. Virus was preincubated with the compounds (individual and mixed) for 45 min at 22 °C, and then added to cells. A standard infection curve was generated in parallel by infecting cells in the absence of compounds using serial twofold dilutions of virus. All reactions were done in triplicate. Cells, virus and compounds were incubated for 48 h at 37 °C and 5% CO_2. Infection, as measured by Ad-mediated GFP expression, was analyzed using a Typhoon 9410 imager (GE Healthcare Life Sciences), and quantified with ImageQuantTL (GE Healthcare Life Sciences). Compounds that showed antiviral activity were further tested in a dosage assay using 15,000 vp/cell and compound concentrations ranging 40–2.5 μM.

2.4. Cytotoxicity assay

The cytotoxicity of the compounds was measured using the XTT-based Cell Proliferation Kit II (Roche) according to the manufacturer's instructions. Actively dividing A549 cells were incubated with compounds for 48 h. After the incubation the XTT reaction mix was added to the cells for an extra 18 h. The 50% cell cytotoxic concentration (CC_{50}) of 15D8 was calculated according to Cheng et al. (2002). The selectivity index (SI) was evaluated as the ratio of CC_{50} to IC_{50}, where the IC50 is defined as the concentration of compound that inhibits Ad infection by 50%.

2.5. Plaque assay

For low MOI infections, active compounds were further evaluated in a plaque assay. 293β5 cells were seeded in 6-well plates at 4×10^5 cells per well in duplicate for each condition. When cells reached 70–80% confluency, they were infected with Ad5-GFP or Ad16-GFP (0.25 vp/cell) and rocked for 2 h at 37 °C. The inoculum was removed and the cells were washed once with PBS. The cells were then carefully overlaid with 4 ml/well of equal parts of Avicel 2.4% (RC-581) and 2× EMEM (BioWhittaker) supplemented with 2× penicillin/streptomycin, 2× L-glutamine and 10% FBS. The mixture also contained compound in concentrations ranging from 5 to 1 μM. Following incubation for 72 h at 37 °C, plates were scanned with a Typhoon 9410 imager (GE Healthcare Life Sciences), and plaques were quantified with ImageJ (Schneider et al., 2012).

2.6. Ad-mediated endosome disruption

To assess endosome disruption in live cells, Ad-mediated ribotoxin (α-sarcin) delivery experiments were performed as previously described (Moyer et al., 2011) with some modifications. Briefly, 10,000 A549 cells were seeded in black 96-well plates and incubated in complete DMEM for 24 h. The cells were washed and then incubated at 37 °C for 1 h in DMEM without cysteine or methionine and supplemented with 10% dialyzed FBS (DMEM-). In parallel, 3-fold serial dilutions (1000–0.02 ng) of Ad5*ts*1 or Ad5-GFP was preincubated with compound 15D8 (40 μM), compound 16D7-16 (40 μM) or the same volume of DMSO (control) for 1 h on ice. Following the incubations, the medium was removed and replaced with 50 μl DMEM-containing 0.1 mg/ml of α-sarcin (Calbiochem/EMD Biosciences, La Jolla, CA) and the virus/compound mixtures. After 2 h at 37 °C, the cells were washed and the medium replaced with DMEM-containing 0.1 μCi/well [^{35}S]-methionine (PerkinElmer) (Smith et al., 2003). After 2 additional hours of incubation at 37 °C, cells were washed twice with PBS and then incubated with 5% trichloroacetic acid for 1 h on ice. The plates were then washed two more times with 100% cold ethanol and air dried overnight. Cell samples were solubilized with 10 μl/well of 1% SDS-0.1 N NaOH for 10 min, neutralized with 2 μl/well of 0.6 N HCl and covered with Microscint-20 (Packard). [^{35}S]-methionine incorporation was measured with a TopCount (Packard) scintillation counter, and calculated by subtracting the background level of a control well containing [^{35}S]-methionine and α-sarcin but not virus.

2.7. DNA and mRNA quantification by real-time PCR

For DNA quantification, A549 cells (25,000 cells/well in a 96 well-plate) were infected with wild type Ad5 or Ad16 (100 vp/cell) and incubated for 2 h at 37 °C in complete DMEM. After

the incubation, excess virus was removed and the medium was replaced with 100 μl of complete DMEM containing 30 μM of either 15D8, negative control compound 16D7-16, or the same volume of DMSO. All samples were done in triplicate. After 24 h of incubation at 37 °C, DNA was purified from the cell lysate with the QIAamp DNA Mini Kit (QIAGEN, Valencia, CA) following the manufacturer's instructions. TaqMan primers and probes for a region of the Ad5 hexon were designed with the GenScript Real-time PCR (TaqMan) Primer Design software (GenScript). Oligonucleotides sequences were AdF: 5′-GACATGACTTTTGAGGTG GA-3′; AdR: 5′-GTGGCGTTGCCGGCCGAGAA-3′; and AdProbe: 5′-TCCATGGGATCCACCTCAAA-3′. Real-time PCR mixtures consisted of 2 μl the purified DNA, AdF and AdR at a concentration of 200 nM each, and AdProbe at a concentration of 50 nM in a total volume of 12.5 μl and mixed with 12.5 μl of KAPA PROBE FAST qPCR Master Mix (KAPABiosystems, MA). The PCR cycling protocol was 95 °C for 3 min followed by 40 cycles of 95 °C for 10 s and 60 °C for 30 s.

For quantification of RNA expression, the conditions of infection were the same used for the DNA quantification. Twenty-four hours after infection RNA was purified with the miRCURY RNA Isolation Kit (Exiqon Inc., MA) following the manufacturer's instructions. Quantification of RNA copy numbers was performed using primers and conditions previously reported for E1A and E2B (Rivera et al., 2004).

Human glyceraldehyde-3-phosphate dehydrogenase (GAPDH) and β-globin genes were used as internal controls. Oligonucleotides sequences for GAPDH and conditions were those previously reported by Rivera et al. (2004). For quantification, gene fragments from hexon and GAPDH were cloned into the pGEM-T Easy vector (Promega) and known concentrations of template were used to generate a standard curve in parallel for each experiment. All assays were performed in a C1000 Thermal Cycler apparatus (BioRad).

2.8. Nuclear-associated Ad genomes

Nuclear delivery of the Ad genome was assessed with real-time PCR following nuclear isolation from infected cells using a previously described protocol with a few modifications (Schreiner et al., 2012). Briefly, 1×10^6 A549 cells in 6-well plates were infected with Ad5 wild type at MOI 2000 vp/cell in the presence of 30 μM of 15D8 or the same volume of DMSO. Forty-five minutes after the infection, cytoplasmic and nuclear fractions were separated using a hypotonic buffer solution and NP-40 detergent. Following infection, A549 cells were trypsinized and collected, and then washed twice with PBS. The cell pellet was resuspended in 500 μl of 1× hypotonic buffer (20 mM Tris–HCl pH 7.4, 10 mM NaCl, 3 mM $MgCl_2$) and incubated for 15 min at 4 °C. Then, 25 μl of NP-40 was added and the samples were vortexed. The homogenates were centrifuged for 10 min at 835×*g* at 4 °C. Following removal of the cytoplasmic fraction (supernatant), DNA was isolated from the nuclear fraction (pellet) using the QIAamp DNA Mini Kit (QIAGEN, Valencia, CA).

2.9. Virus yield reduction by piperazinone 15D8

The effect of 15D8 on virus production was evaluated in a burst assay. A549 cells were infected with wild-type Ad5 or Ad16 (MOI 100) in the presence or absence of 30 μM compound 15D8. After 48 h, cells were harvested and subjected to three rounds of freeze/thaw. Serial dilutions of clarified lysates were titrated on A549 cells and $TCID_{50}$ values were calculated using an endpoint dilution method (Reed and Muench, 1938).

2.10. Human cytomegalovirus (HCMV) infectivity assay by quantitative real-time PCR

To test the sensitivity of HCMV to 15D8, MRC-5 cells (1.75×10^5 cells/well in a 6-well plate) were infected with HCMV at an MOI of 0.05 vp/cell and incubated in complete DMEM supplemented with 30 μM of 15D8 or the same volume of DMSO in triplicate. After 24 h of incubation at 37 °C, DNA was purified from the cell lysate with the QIAamp DNA Mini Kit (QIAGEN, Valencia, CA) following the manufacturer's instructions. qPCR was performed using the RealStar CMV PCR Kit 1.2 (Altona Diagnostics, Hamburg, Germany) following the manufacturer's instructions.

2.11. Statistical analyses

Statistical analyses were performed with the GraphPad Prism 5 suite using one-way analysis of variance, including a Dunnett post-test. Unless otherwise indicated, data are presented as the mean of triplicate samples ± standard deviation (SD). *P*-values are indicated when statistically significant.

3. Results

3.1. High-throughput screening (HTS) of combinatorial chemical libraries

The generation of libraries of chemically synthesized small molecules that were designed to disrupt protein–protein interactions (Boger et al., 2003; Lee et al., 2008; Shaginian et al., 2009; Whitby et al., 2011; Whitby and Boger, 2012) provided a unique opportunity to screen a large number of compounds for inhibitors of Ad5 infection by modulating key protein–protein or protein–nucleic acid interactions. We used HTS to assess more than 25,000 different compounds at an initial concentration of 50 μM, presented as either a single molecule or a small mixture of compounds.

A number of active compounds were identified within a 150-member sublibrary of trisubstituted piperazin-2-one derivatives screened as pure individual compounds (Boger et al., 2000; Lee et al., 2008; Whitby et al., 2009). From this sublibrary, our primary screen identified 28 compounds that inhibited Ad5 infection >50%. The active compounds were further evaluated for effects on cellular viability (excluding those that were found to be cytotoxic), for measurement of IC_{50} values (Table 1) and also to gain some mechanistic understanding for inhibition. Analysis of these hits demonstrated clear structure–activity relationship (SAR) trends (Fig. 1), which is suggestive of inhibitory activity derived from interaction with a specific protein target. The majority of piperazin-2-one compounds screened were racemic at C6 of the piperazinone ring (R^1 position), but screening of a set of compounds containing the (S)-configuration at R^1 provided active compounds, suggesting that the (S)-enantiomer is the active configuration. To quantitatively assess and depict the SAR trends, each side chain entity represented in the piperazin-2-one library at the R^1 position was scored as the sum average % inhibition of all compounds containing that side chain at R^1 (Fig. 1, black bars). Thus, each of the black bars

Table 1
Piperazinone 15D8 IC_{50}, CC_{50} and SI values.

	MOI	IC_{50} (μM)	CC_{50} (μM)	Selective index (SI)
Ad5-GFP	15,000	19.2 ± 0.87	194 ± 15.3	10.1
Ad5	0.25	1.3 ± 0.18		149
Ad16-GFP	15,000	37.9 ± 1.78		5.1
Ad16	0.25	0.8 ± 0.74		242

in the R^1 position bar graph in Fig. 1 constitutes the average % inhibition of the 50 compounds in the library containing the specified R^1 side chain (ethyl, benzyl, or phenethyl). This method revealed that an ethyl group is strongly favored at this position. Performing the same analysis at R^2 (average % inhibition of 30 compounds for each bar) demonstrated that a 4-OMe benzyl group was preferred, with the other 4-substituted benzyl side chains (4-Cl, 4-Me) also showing strong activity (Fig. 1, blue bars). At the R^3 position (average % inhibition of 15 compounds for each bar) the analysis revealed that the presence of a 2-benzofuran side chain resulted in the best activity, followed by the 4-Cl phenyl and 2-benzothiophene moieties (Fig. 1, red bars). Beautifully, combining the best-performing side chain at each position from the sum average SAR analysis results in the structure of compound 15D8, which was identified in secondary screening as the most potent piperazin-2-one inhibitor (Fig. 1).

Piperazinone 15D8 reproducibly inhibited Ad5 infection in a dose-dependent manner at high MOI (15,000 vp/cell) (Fig. 2A) without causing measurable cytotoxicity. In secondary screening assays using a low input of virus (0.25 vp/cell), 15D8 also showed dose-dependent activity with 100% inhibition of plaque formation at concentrations higher than 3 μM (Fig. 2C). We also tested the antiviral activity of 15D8 against a species B Ad (Ad16), and found similar levels of inhibition to those seen with Ad5 (Fig. 2B and D). The IC_{50} values for 15D8 against Ad5 and Ad16 are summarized in Table 1.

In an assay measuring antiviral activity as a function of MOI, inhibition by 30 μM 15D8 was inversely proportional to the number of input particles at very low MOI (Fig. S1A). While 15D8 was also inhibitory at high MOI, the relationship between the number of infecting virus particles and compound concentration is less marked, as expected (Fig. S1B).

We also analyzed the cellular cytotoxicity of piperazinone 15D8. At concentrations $\leqslant$30 μM, 58 did not significantly alter cell viability as determined by the XTT metabolic assay. The CC_{50} for compound 15D8 was 194 μM (Table 1), significantly higher than the 30 μM concentration required for inhibition in our mechanistic assays.

3.2. Impact of piperazinone 15D8 on Ad entry

Our infection assays indicated that treatment with 15D8 was inhibiting expression of the Ad5-GFP and Ad16-GFP transgenes, but did not give any indication of the mechanism of inhibition.

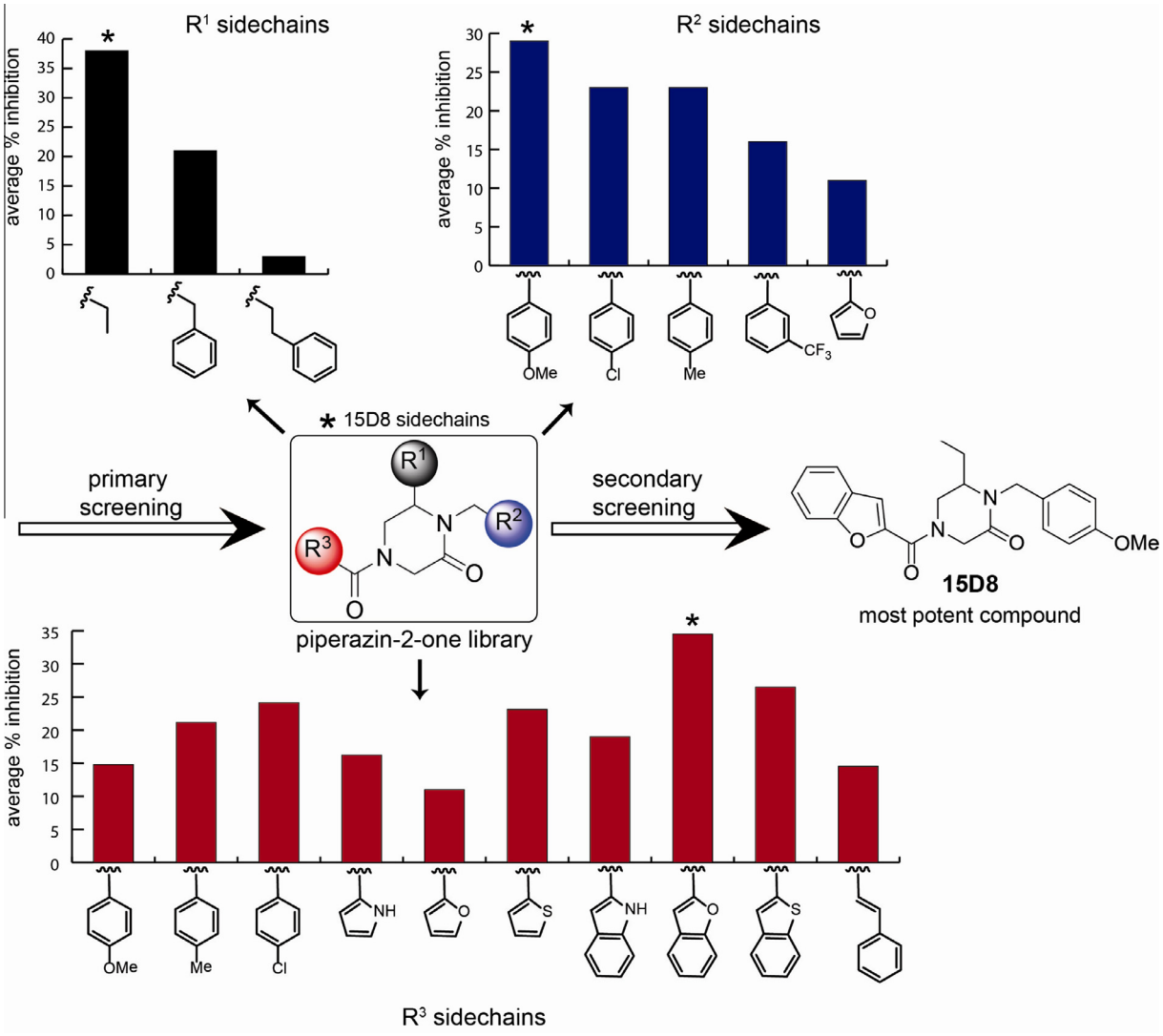

Fig. 1. SAR analysis from screening of the piperazin-2-one sublibrary and discovery of compound 15D8. The SAR trends are assessed and depicted using an average % inhibition bar graph analysis, wherein each bar value is determined by calculating the sum average % inhibition of all compounds in the piperazin-2-one library (150 compounds) containing the specified side chain (*x*-axis) at the indicated position (R^1, R^2, or R^3). Further analysis of active compounds (secondary screening) led to the identification of piperazinone 15D8 as the most potent inhibitor.

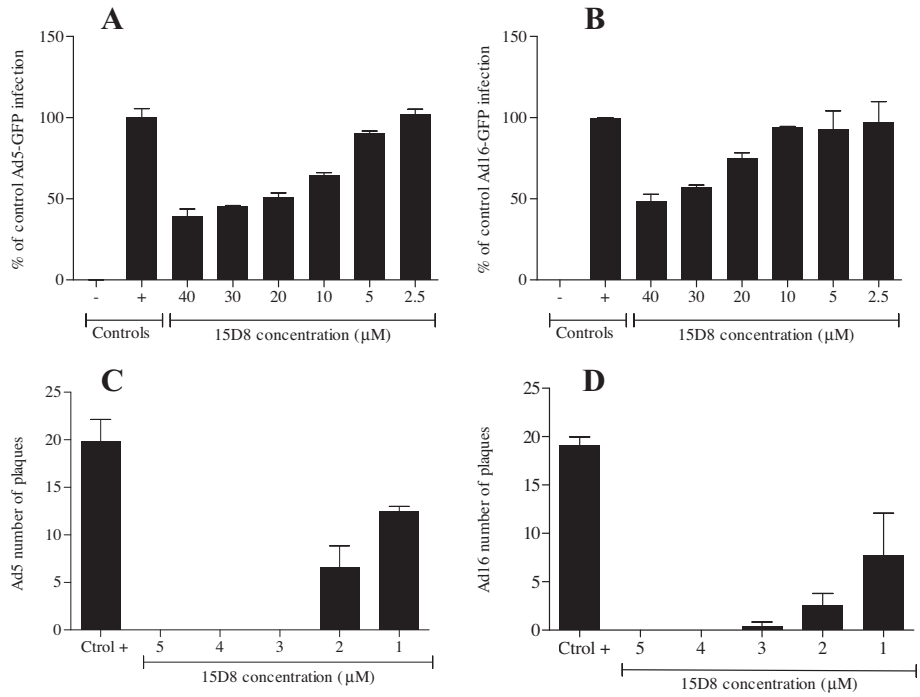

Fig. 2. Inhibitory activity of piperazinone 15D8. Dose-dependent activity of 15D8 against Ad5-GFP (A) and Ad16-GFP (B) in a high MOI single round infection assay using A549 cell. Antiviral effects of compound 15D8 at low MOI on Ad5 (C) and Ad16 (D) in a plaque assay using the 293β5 cell line. For all panels, the negative control (−) is non-infected cells, while the positive control (+) is cells infected at the same MOI but in absence of compound. Data are presented as the mean ± SD from triplicate assays.

The Ad cell entry pathway is a highly coordinated multi-stage process, and interference at any of these steps would ultimately result in decreased GFP expression. Thus, we investigated several cell entry points, including virus cell attachment and particle internalization, but saw no effect for either of these steps in the presence of 15D8 (data not shown). We next tested the compounds in a physiological assay involving Ad-mediated co-delivery of a ribotoxin (α-sarcin) in live cells as an indication of the ability of the compounds to influence virus-mediated endosomolysis (Smith and Nemerow, 2008; Wiethoff et al., 2005). Ad-mediated endosome disruption results in cytosolic ribotoxin delivery and decreased host protein synthesis. We did not detect a significant change in the ID_{50} (50% inhibitory dose) for Ad-mediated endosome penetration in the presence of 15D8 (Fig. S2) compared to DMSO or the negative control compound 16D7-16, a closely related trisubstituted piperazin-2-one that lacks anti-adenovirus activity (Fig. 4B). Neither of these conditions altered endosome disruption. In contrast, Ad5*ts1*, an endosome penetration-defective mutant virus, exhibited a 70-fold increase in the ID_{50} with respect to the DMSO control (Fig. S2).

3.3. Impact of piperazinone 15D8 on Ad genome accessibility to the nucleus

Since our results indicated 15D8 did not affect any step of cell entry up to and including Ad-mediated endosome rupture, we next wanted to test if the compound affected nuclear delivery of the Ad genome. After protein VI-mediated endosome lysis and subsequent endosomal escape, partially uncoated Ad capsids are transported to the nuclear envelope via microtubules (Bremner et al., 2009). Subsequently, the Ad genome, along with protein VII, is imported into the nucleus via the nuclear pore complex (Strunze et al., 2011). We reasoned that 15D8 might inhibit the transport of partially disassembled Ad capsids from the endosomes to the nucleus or disrupt genome nuclear translocation. Therefore, we used an assay to quantify nuclear delivery of the Ad genome. At 45 min post-infection, there was no significant difference in the amount of Ad DNA isolated from the nucleus of cells treated with 15D8 versus those treated with DMSO (Fig. 3A). As a control for the purity of nuclear isolation, we also measured the DNA copy number of the cellular housekeeping gene GAPDH in both the nucleus and the cytoplasm. These results indicate that we were specifically measuring Ad DNA that reached the nucleus (Fig. 3B) and that the compound did not alter any of the steps leading up to this late entry event. Therefore we sought to determine if a later step(s) in the virus life cycle was affected by 15D8.

3.4. Piperazinone 15D8 impacts Ad replication

Thus, the next step was to examine the effect that compound 15D8 had on virus replication using a virus burst assay which measures the production of virus particles. As summarized in Table S1, treatment with 15D8 was associated with overall reductions in virus yield of 12–17-fold for Ad5 and 5–15-fold for Ad16. As viral replication is dependent upon efficient DNA replication, we performed quantitative real-time PCR (qPCR) to measure Ad DNA replication in the presence of 15D8. Ad-infected A549 cells were incubated for 24 h at 37 °C before washing to remove unbound virions. DNA was extracted at this early time point to avoid the influence of newly generated viral particles derived from subsequent rounds of infection occurring 32–36 h post infection (Horwitz, 1991). Quantitative PCR has been previously used to examine the susceptibility of Ad to potential antiviral agents, primarily nucleoside and nucleotide analogs (Gainotti et al., 2010; Naesens et al., 2005). Here, we used a similar approach but processed our samples at an earlier time point, thus quantifying the production of new Ad DNA copies in a single round of infection as a measure of DNA replication efficiency. The presence of 15D8 at 30 μM concentration significantly inhibited ($p < 0.05$, Dunnett's Multiple Comparison test) Ad DNA replication by more than 50%,

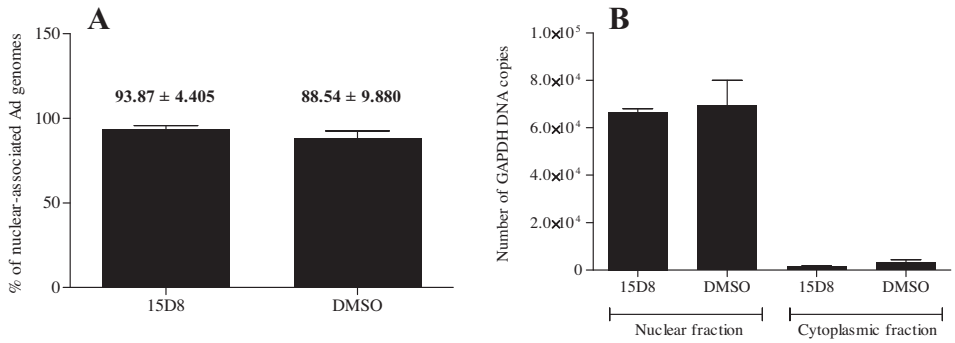

Fig. 3. Nuclear association of Ad DNA. (A) The presence of 15D8 (30 μM) did not alter the access of Ad genomes to the nucleus. (B) Control for the specificity of nuclear DNA purification. The results represent means ± SD of triplicate samples from two independent experiments.

with no significant effect on cellular control genes GAPDH and β-globin (Figs. 4A and B and S3). As expected, the negative control compound 16D7-16 had no effect on Ad DNA replication (Fig. 4A and B).

The decrease in Ad DNA copy number at the nucleus 24 hpi in the presence of 15D8 suggests two possibilities for the precise mechanism of inhibition. First, 15D8 could inhibit Ad DNA replication directly by interfering with a protein involved in this process, such as the Ad DNA polymerase. Alternatively, 15D8 may impact transcription of the Ad immediate early and early genes, which is a prerequisite for subsequent DNA replication.

To assay the inhibition of Ad mRNA transcription by 15D8, we infected A549 cells in the presence of the compound (30 μM) for 6 h and 24 h. After the infection, we quantified the mRNA copy number of an immediate early gene (E1A) and an early gene (E2B) using quantitative reverse transcription (RT-PCR). As shown in Fig. 5, there were no significant differences in total mRNA levels for E1A or E2B at 6 hpi. However, at 24 hpi, we observed a significant decrease in mRNA copy number for both E1A and E2B in the presence of 15D8, but not 16D7-16. Compound 15D8 did not significantly impact GAPDH mRNA levels at either time point (data not shown). The ability of 15D8 to alter Ad early gene transcription at the later time point is consistent with a block in DNA replication that indirectly impacts transcription.

3.5. Piperazinone 15D8 does not restrict HCMV infection

Given that other antiviral compounds such as nucleotide and nucleoside analogs (i.e., cidofovir) have been shown to have broad activity against multiple dsDNA virus including HCMV and Ad via blockage of viral DNA polymerases (Lindemans et al., 2010), we explored the possible inhibitory activity of 15D8 on HCMV DNA replication. Quantification of total HCMV DNA 24 h after infection of MRC-5 cells revealed no differences between samples treated with our hit compound and those treated with the same volume of DMSO (Fig. 4C). Quantitative PCR for the GAPDH gene was included as control, again showing no differences between samples (data not shown). Together, these results suggest a specific mechanism for the inhibition of Ad infection involving the machinery that participates in Ad DNA replication.

4. Discussion and conclusion

The original goal of this study was to identify small molecule inhibitors of Ad disassembly or membrane penetration during cell entry. As endosome disruption is dependent upon exposure of a predicted N-terminal amphipathic α-helix of protein VI (Wiethoff et al., 2005), we wished to identify a small compound that prevented the release or altered the functionality of protein VI. We selected libraries for screening based on their ability to disrupt protein–protein interactions via interaction with α-helix and β-turn structures.

Using HTS of combinatorial chemical libraries combined with functional assays, we identified a hit piperazin-2-one, 15D8, which substantially inhibited expression of the Ad-GFP transgene in cell culture. The compound exhibited modest inhibition of Ad5-GFP and Ad16-GFP infection at high MOI as measured by Ad-mediated GFP expression but displayed even more potent activity when tested at low MOI. The piperazinone 15D8 was derived from a library that was previously found to contain synthetic molecules with antiviral activity against human arenaviruses (Lee et al., 2008). However, the piperazin-2-one that was active against arenavirus did not inhibit Ad infection, highlighting its virus-specific function. The proposed mechanism of action of these arenavirus specific piperazin-2-ones was disruption of virion escape from the endosome to the cytosol, specifically at the level of glycoprotein (GP)-mediated membrane fusion with the endosomal membrane at low pH (pH 5.0) (Lee et al., 2008). Interestingly, our findings showed that for both of these different viruses, the most powerful antiviral compounds required the 2-benzofuran aryl substituent together with the piperazine-2-one core structure, with the substituent at N^1 acting as a modulator of the activity (Lee et al., 2008). However, in the arenavirus inhibitors, a C6 benzyl or phenethyl substituent resulted in the most potent compounds. Those substituents led to inactive compounds against Ad, as an ethyl group at C6 was strictly required for strong activity. Thus, even though 15D8 was derived from the same small molecule library and is closely related, its SAR and mechanism of action against enveloped (arenavirus) and non-enveloped virus (Ad) appear to be distinct.

Following receptor engagement by the fiber, Ad5 and Ad16 particles are internalized by receptor-mediated endocytosis, a process that requires the Ad penton base and cellular αvβ3 or αvβ5 integrins (Smith et al., 2003; Tomko et al., 1997; Wickham et al., 1993). Once inside the endosome, capsids undergo partial disassembly and release several viral proteins, including the membrane lytic protein VI. Following endosomolysis, the virus escapes to the cytoplasm (Wiethoff et al., 2005), where the partially uncoated capsid is transported via microtubules to the nuclear envelope. Ad genomic DNA, together with protein VII, is then translocated through the nuclear pore complex (Greber et al., 1993; Smith et al., 2008; Trotman et al., 2001). We demonstrated that 15D8 did not inhibit any step of the cell entry process up to DNA delivery to the nucleus. Ad entered the cell and escaped from the endosome with no interference of the compound, and the Ad DNA accumulated at the nucleus of the cell host normally. Currently, we cannot formally exclude the possibility that the compound restricts arrival of the viral genome at the proper location within the nucleus.

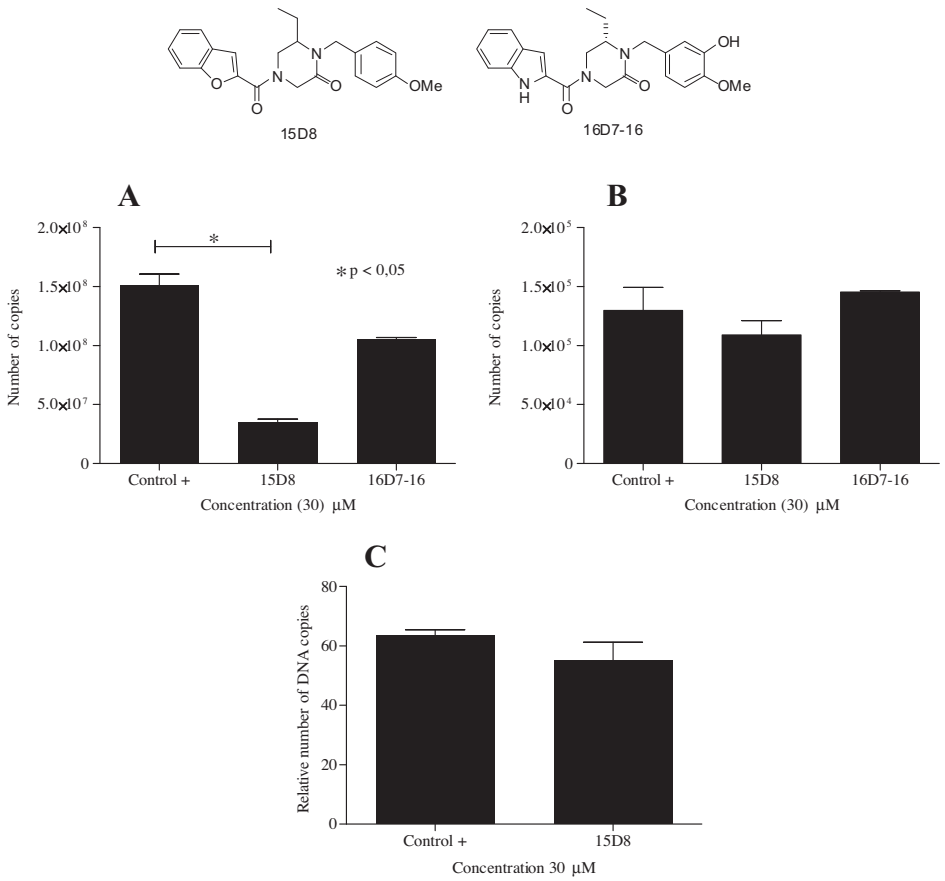

Fig. 4. Piperazinone 15D8 inhibits DNA replication for Ad5 but not HCMV. (A) 15D8, but not 16D7-16, significantly reduced *de novo* production of Ad5 DNA copies compared to a positive control 24 h post-infection in a quantitative PCR assay. (B) The levels of cellular GAPDH did not show a significant difference among the three conditions. Control samples are infected cells in the presence of an equivalent volume of DMSO as that used for the compounds. (C) The relative copy number of HCMV DNA was measured by qPCR at 24 hpi. For all panels, the results represent means ± SD of triplicate assays.

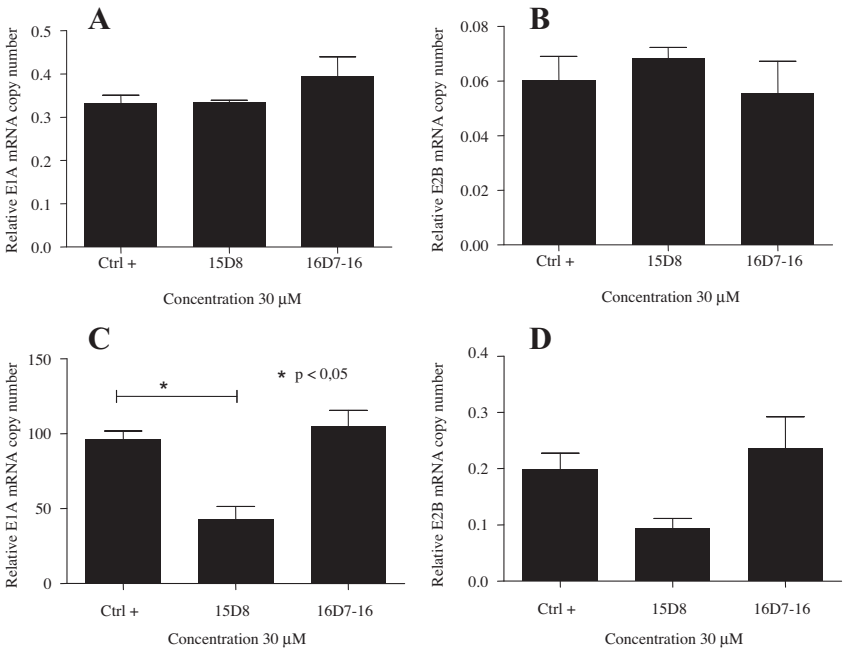

Fig. 5. Effect of piperazinone 15D8 on mRNA transcription of Ad early genes. Relative copy numbers of E1A (Panels A and C) and E2B (Panels B and D) mRNA were measured in the presence of DMSO, 15D8, or the non-inhibitory 16D7. Samples were collected and processed at either 6 hpi (Panel A and B) or 24 hpi (Panel C and D). Results are expressed as the relative copy number of E1A/E2B mRNA normalized to GAPDH copy number and are presented as the mean ± SD from triplicate assays.

Our results show clear inhibition of Ad DNA replication with no effect on the transcription of the Ad E1A and E2B genes at 6 hpi. Prior to Ad DNA replication, the transcription of E1A by cellular RNA polymerase II takes place from the E1A promoter (Pettersson and Roberts, 1986). The E1A protein further promotes its own transcription and is necessary for both the subsequent expression of the early genes E1B, E2, E3 and E4 from different promoters and for Ad DNA replication. A reasonable explanation for the decrease in Ad mRNA transcription at 24 hpi in the presence of 15D8 is the reduction in total Ad DNA templates, which is consistent with the inhibitory effect of 15D8 on viral DNA replication.

Once the Ad DNA–pVII complex enters the nucleus, it forms a chromatin-like structure that must be relaxed and remodeled to allow for expression of Ad genes. The role of protein VII on Ad DNA transcription/replication remains a highly controversial issue, specifically regarding the timing and nature of protein VII dissociation from the Ad genome (Komatsu et al., 2011; Xue et al., 2005). Studies suggest that a mechanism requiring ongoing transcription is responsible for the release of protein VII, probably mediated by E1A (Chen et al., 2007). The Ad DNA–pVII condensed structure does not allow for an efficient transcription and DNA replication as previously probed in *in vitro* studies (Giberson et al., 2012; Okuwaki and Nagata, 1998). Three cellular proteins, template activating factors (TAF) Iβ, II and III, have been implicated in remodeling the Ad DNA–pVII complex to enhance Ad DNA processing efficiency (Giberson et al., 2012). The mechanism by which those cellular proteins, particularly the well-characterized TAF Iβ, help remodel the Ad DNA–pVII complex implies direct binding to the complex, favoring the relaxation of that structure and allowing access to the replication machinery. However, it is still not clear if the activity of TAF Iβ requires prior dissociation of protein VII from Ad DNA. In any case, protein VII is a crucial factor in controlling Ad DNA transcription and genome replication. Taken together, it is reasonable to assume that regardless of the precise mechanism, the association of protein VII with Ad DNA would be lower or more relaxed, at least immediately after the Ad genome enters the nucleus. This would allow transcription of E1A mRNA early after nuclear entry and ultimately, a cascade of transcription events that culminates in viral protein expression, and DNA replication.

Several scenarios may account for our findings that 15D8 interferes with DNA replication. It is possible 15D8 strengthens the DNA–VII complex, thereby stabilizing the Ad chromatin structure and blocking access by the replication machinery. Alternatively, compound 15D8 may interact with viral proteins essential for DNA replication, including precursor of the terminal protein (pTP), Ad DNA polymerase or the DNA-binding protein (DBP). Further studies will be needed to clarify the specific mechanism for 15D8 inhibition of Ad DNA replication. This compound could therefore be a useful tool to unravel the complex events involved in Ad DNA replication.

Piperazinone 15D8 has proven to be a significant inhibitor of Ad infection targeting Ad DNA replication. Although further optimization and evaluation will be required for this compound, it could potentially represent a strong hit compound for the treatment of Ad infections in immunosuppressed patients. Further studies using 15D8 in an animal model of Ad infection should improve our knowledge of its efficacy in vivo, as well as providing additional information on bioavailability, pharmacokinetics and safety.

Acknowledgments

Supported by Plan Nacional de I+D+i 2008-2011 and Instituto de Salud Carlos III, Subdirección General de Redes y Centros de Investigación Cooperativa, Ministerio de Economía y Competitividad, Spanish Network for Research in Infectious Diseases (REIPI RD12/0015) – co-financed by European Development Regional Fund "A way to achieve Europe" ERDF and by Andalusia Health and Social Welfare Ministry (PI-0058-2012). J.S.C. is supported by a post-doctoral contract Sara Borrell from the Instituto de Salud Carlos III (CD10/00280). The work was also supported by NIH grants HL054352 to G.R.N. and CA042056 to D.L.B. This is manuscript # 26010 at The Scripps Research Institute.

Appendix A. Supplementary data

Supplementary data associated with this article can be found, in the online version, at http://dx.doi.org/10.1016/j.antiviral.2014.05.010.

References

Boger, D.L., Tarby, C.M., Myers, P.L., Caporale, L.H., 1996. Generalized dipeptidomimetic template: solution phase parallel synthesis of combinatorial libraries. J. Am. Chem. Soc. 118, 2109–2110.
Boger, D.L., Goldberg, J., Satoh, S., Ambroise, Y., Cohen, S.B., Vogt, P.K., 2000. Non-amide-based combinatorial libraries derived from N-Boc-iminodiacetic acid: solution-phase synthesis of piperazinone libraries with activity against LEF-1/beta-catenin-mediated transcription. Helv. Chim. Acta 83, 1825–1845.
Boger, D.L., Desharnais, J., Capps, K., 2003. Solution-phase combinatorial libraries: modulating cellular signaling by targeting protein–protein or protein–DNA interactions. Angew. Chem. Int. Ed. Engl. 42, 4138–4176.
Bremner, K.H., Scherer, J., Yi, J., Vershinin, M., Gross, S.P., Vallee, R.B., 2009. Adenovirus transport via direct interaction of cytoplasmic dynein with the viral capsid hexon subunit. Cell Host Microbe 6, 523–535.
Chen, J., Morral, N., Engel, D.A., 2007. Transcription releases protein VII from adenovirus chromatin. Virology 369, 411–422.
Cheng, S., Comer, D.D., Williams, J.P., Myers, P.L., Boger, D.L., 1996. Novel solution phase strategy for the synthesis of chemical libraries containing small organic molecules. J. Am. Chem. Soc. 118, 2567–2573.
Cheng, H.Y., Lin, C.C., Lin, T.C., 2002. Antiherpes simplex virus type 2 activity of casuarinin from the bark of *Terminalia arjuna* Linn. Antiviral Res. 55, 447–455.
Cianci, C., Langley, D.R., Dischino, D.D., Sun, Y., Yu, K.L., Stanley, A., Roach, J., Li, Z., Dalterio, R., Colonno, R., Meanwell, N.A., Krystal, M., 2004. Targeting a binding pocket within the trimer-of-hairpins: small-molecule inhibition of viral fusion. Proc. Natl. Acad. Sci. U.S.A. 101, 15046–15051.
Echavarria, M., 2008. Adenoviruses in immunocompromised hosts. Clin. Microbiol. Rev. 21, 704–715.
Este, J.A., Telenti, A., 2007. HIV entry inhibitors. Lancet 370, 81–88.
Frey, G., Rits-Volloch, S., Zhang, X.Q., Schooley, R.T., Chen, B., Harrison, S.C., 2006. Small molecules that bind the inner core of gp41 and inhibit HIV envelope-mediated fusion. Proc. Natl. Acad. Sci. U.S.A. 103, 13938–13943.
Gainotti, R., Ricarte, C., Ebekian, B., Videla, C., Carballal, G., Damonte, E.B., Echavarria, M., 2010. Real time PCR for rapid determination of susceptibility of adenovirus to antiviral drugs. J. Virol. Methods 164, 30–34.
Giberson, A.N., Davidson, A.R., Parks, R.J., 2012. Chromatin structure of adenovirus DNA throughout infection. Nucleic Acids Res. 40, 2369–2376.
Greber, U.F., Willetts, M., Webster, P., Helenius, A., 1993. Stepwise dismantling of adenovirus 2 during entry into cells. Cell 75, 477–486.
Horwitz, M.S., 1991. Adenoviridae and their replication. In: Fields, B.N., Knipe, D.M., Chanock, R.M., et al. (Eds.), Virology, second ed. Raven Press, New York, NY, pp. 771–813.
Humar, A., Kumar, D., Mazzulli, T., Razonable, R.R., Moussa, G., Paya, C.V., Covington, E., Alecock, E., Pescovitz, M.D., 2005. A surveillance study of adenovirus infection in adult solid organ transplant recipients. Am. J. Transplant. 5, 2555–2559.
Ison, M.G., Green, M., 2009. Adenovirus in solid organ transplant recipients. Am. J. Transplant. 9 (Suppl. 4), S161–S165.
Komatsu, T., Haruki, H., Nagata, K., 2011. Cellular and viral chromatin proteins are positive factors in the regulation of adenovirus gene expression. Nucleic Acids Res. 39, 889–901.
Lee, A.M., Rojek, J.M., Spiropoulou, C.F., Gundersen, A.T., Jin, W., Shaginian, A., York, J., Nunberg, J.H., Boger, D.L., Oldstone, M.B., Kunz, S., 2008. Unique small molecule entry inhibitors of hemorrhagic fever arenaviruses. J. Biol. Chem. 283, 18734–18742.
Lenaerts, L., De Clercq, E., Naesens, L., 2008. Clinical features and treatment of adenovirus infections. Rev. Med. Virol. 18, 357–374.
Lindemans, C.A., Leen, A.M., Boelens, J.J., 2010. How I treat adenovirus in hematopoietic stem cell transplant recipients. Blood 116, 5476–5485.
Morfin, F., Dupuis-Girod, S., Mundweiler, S., Falcon, D., Carrington, D., Sedlacek, P., Bierings, M., Cetkovsky, P., Kroes, A.C., van Tol, M.J., Thouvenot, D., 2005. In vitro susceptibility of adenovirus to antiviral drugs is species-dependent. Antivir. Ther. 10, 225–229.
Morfin, F., Dupuis-Girod, S., Frobert, E., Mundweiler, S., Carrington, D., Sedlacek, P., Bierings, M., Cetkovsky, P., Kroes, A.C., van Tol, M.J., Thouvenot, D., 2009. Differential susceptibility of adenovirus clinical isolates to cidofovir and ribavirin is not related to species alone. Antivir. Ther. 14, 55–61.

Moyer, C.L., Wiethoff, C.M., Maier, O., Smith, J.G., Nemerow, G.R., 2011. Functional genetic and biophysical analyses of membrane disruption by human adenovirus. J. Virol. 85, 2631–2641.
Naesens, L., Lenaerts, L., Andrei, G., Snoeck, R., Van Beers, D., Holy, A., Balzarini, J., De Clercq, E., 2005. Antiadenovirus activities of several classes of nucleoside and nucleotide analogues. Antimicrob. Agents Chemother. 49, 1010–1016.
Nepomuceno, R.R., Pache, L., Nemerow, G.R., 2007. Enhancement of gene transfer to human myeloid cells by adenovirus–fiber complexes. Mol. Ther. 15, 571–578.
Nguyen, E.K., Nemerow, G.R., Smith, J.G., 2010. Direct evidence from single-cell analysis that human {alpha}-defensins block adenovirus uncoating to neutralize infection. J. Virol. 84, 4041–4049.
Okuwaki, M., Nagata, K., 1998. Template activating factor-I remodels the chromatin structure and stimulates transcription from the chromatin template. J. Biol. Chem. 273, 34511–34518.
Paolino, K., Sande, J., Perez, E., Loechelt, B., Jantausch, B., Painter, W., Anderson, M., Tippin, T., Lanier, E.R., Fry, T., DeBiasi, R.L., 2011. Eradication of disseminated adenovirus infection in a pediatric hematopoietic stem cell transplantation recipient using the novel antiviral agent CMX001. J. Clin. Virol. 50, 167–170.
Pettersson, U., Roberts, R.J., 1986. Adenovirus gene expression and replication: a historical review. In: DNA Tumor Viruses: Control of Gene Expression and Replication. Cold Spring Harbor Laboratory, Cold Spring Harbor, NY, pp. 37–57.
Plemper, R.K., Erlandson, K.J., Lakdawala, A.S., Sun, A., Prussia, A., Boonsombat, J., Aki-Sener, E., Yalcin, I., Yildiz, I., Temiz-Arpaci, O., Tekiner, B., Liotta, D.C., Snyder, J.P., Compans, R.W., 2004. A target site for template-based design of measles virus entry inhibitors. Proc. Natl. Acad. Sci. U.S.A. 101, 5628–5633.
Razonable, R.R., Eid, A.J., 2009. Viral infections in transplant recipients. Minerva Med. 100, 479–501.
Reed, L.V., Muench, H., 1938. A simple method of estimating fifty percent endpoints. Am. J. Hyg. 27, 4.
Rivera, A.A., Wang, M., Suzuki, K., Uil, T.G., Krasnykh, V., Curiel, D.T., Nettelbeck, D.M., 2004. Mode of transgene expression after fusion to early or late viral genes of a conditionally replicating adenovirus via an optimized internal ribosome entry site in vitro and in vivo. Virology 320, 121–134.
Robinson, C.M., Singh, G., Lee, J.Y., Dehghan, S., Rajaiya, J., Liu, E.B., Yousuf, M.A., Betensky, R.A., Jones, M.S., Dyer, D.W., Seto, D., Chodosh, J., 2013. Molecular evolution of human adenoviruses. Sci. Rep. 3, 1812.
Schneider, C.A., Rasband, W.S., Eliceiri, K.W., 2012. NIH Image to ImageJ: 25 years of image analysis. Nat. Methods 9, 671–675.
Schreiner, S., Martinez, R., Groitl, P., Rayne, F., Vaillant, R., Wimmer, P., Bossis, G., Sternsdorf, T., Marcinowski, L., Ruzsics, Z., Dobner, T., Wodrich, H., 2012. Transcriptional activation of the adenoviral genome is mediated by capsid protein VI. PLoS Pathog. 8, e1002549.
Shaginian, A., Whitby, L.R., Hong, S., Hwang, I., Farooqi, B., Searcey, M., Chen, J., Vogt, P.K., Boger, D.L., 2009. Design, synthesis, and evaluation of an alpha-helix mimetic library targeting protein–protein interactions. J. Am. Chem. Soc. 131, 5564–5572.
Smith, J.G., Nemerow, G.R., 2008. Mechanism of adenovirus neutralization by Human alpha-defensins. Cell Host Microbe 3, 11–19.
Smith, T.A., Idamakanti, N., Rollence, M.L., Marshall-Neff, J., Kim, J., Mulgrew, K., Nemerow, G.R., Kaleko, M., Stevenson, S.C., 2003. Adenovirus serotype 5 fiber shaft influences in vivo gene transfer in mice. Hum. Gene Ther. 14, 777–787.
Smith, J.G., Cassany, A., Gerace, L., Ralston, R., Nemerow, G.R., 2008. Neutralizing antibody blocks adenovirus infection by arresting microtubule-dependent cytoplasmic transport. J. Virol. 82, 6492–6500.
Stover, J.S., Shi, J., Jin, W., Vogt, P.K., Boger, D.L., 2009. Discovery of inhibitors of aberrant gene transcription from libraries of DNA binding molecules: inhibition of LEF-1-mediated gene transcription and oncogenic transformation. J. Am. Chem. Soc. 131, 3342–3348.
Strunze, S., Engelke, M.F., Wang, I.H., Puntener, D., Boucke, K., Schleich, S., Way, M., Schoenenberger, P., Burckhardt, C.J., Greber, U.F., 2011. Kinesin-1-mediated capsid disassembly and disruption of the nuclear pore complex promote virus infection. Cell Host Microbe 10, 210–223.
Tebruegge, M., Curtis, N., 2012. Adenovirus: an overview for pediatric infectious diseases specialists. Pediatr. Infect. Dis. J. 31, 626–627.
Tomko, R.P., Xu, R., Philipson, L., 1997. HCAR and MCAR: the human and mouse cellular receptors for subgroup C adenoviruses and group B coxsackieviruses. Proc. Natl. Acad. Sci. U.S.A. 94, 3352–3356.
Toth, K., Spencer, J.F., Dhar, D., Sagartz, J.E., Buller, R.M., Painter, G.R., Wold, W.S., 2008. Hexadecyloxypropyl-cidofovir, CMX001, prevents adenovirus-induced mortality in a permissive, immunosuppressed animal model. Proc. Natl. Acad. Sci. U.S.A. 105, 7293–7297.
Trotman, L.C., Mosberger, N., Fornerod, M., Stidwill, R.P., Greber, U.F., 2001. Import of adenovirus DNA involves the nuclear pore complex receptor CAN/Nup214 and histone H1. Nat. Cell Biol. 3, 1092–1100.
Verdeguer, A., de Heredia, C.D., Gonzalez, M., Martinez, A.M., Fernandez-Navarro, J.M., Perez-Hurtado, J.M., Badell, I., Gomez, P., Gonzalez, M.E., Munoz, A., Diaz, M.A., 2011. Observational prospective study of viral infections in children undergoing allogeneic hematopoietic cell transplantation: a 3-year GETMON experience. Bone Marrow Transplant. 46, 119–124.
Whitby, L.R., Boger, D.L., 2012. Comprehensive peptidomimetic libraries targeting protein–protein interactions. Acc. Chem. Res. 45, 1698–1709.
Whitby, L.R., Lee, A.M., Kunz, S., Oldstone, M.B., Boger, D.L., 2009. Characterization of lassa virus cell entry inhibitors: determination of the active enantiomer by asymmetric synthesis. Bioorg. Med. Chem. Lett. 19, 3771–3774.
Whitby, L.R., Ando, Y., Setola, V., Vogt, P.K., Roth, B.L., Boger, D.L., 2011. Design, synthesis, and validation of a beta-turn mimetic library targeting protein–protein and peptide–receptor interactions. J. Am. Chem. Soc. 133, 10184–10194.
Wickham, T.J., Mathias, P., Cheresh, D.A., Nemerow, G.R., 1993. Integrins alpha v beta 3 and alpha v beta 5 promote adenovirus internalization but not virus attachment. Cell 73, 309–319.
Wiethoff, C.M., Wodrich, H., Gerace, L., Nemerow, G.R., 2005. Adenovirus protein VI mediates membrane disruption following capsid disassembly. J. Virol. 79, 1992–2000.
Xue, Y., Johnson, J.S., Ornelles, D.A., Lieberman, J., Engel, D.A., 2005. Adenovirus protein VII functions throughout early phase and interacts with cellular proteins SET and pp32. J. Virol. 79, 2474–2483.